Electronic Supplementary Information

Ultrahigh energy density of a N, O codoped carbon nanosphere based all-solid-state symmetric supercapacitor

Ziyang Song,[a] Dazhang Zhu,[a] Liangchun Li,*[a] Tao Chen,[a] Hui Duan,[a] Zhiwei Wang,[b] Yaokang Lv,[c] Wei Xiong,[d] Mingxian Liu,*[a] and Lihua Gan*[a]

[a] Shanghai Key Lab of Chemical Assessment and Sustainability, School of Chemical Science and Engineering, Tongji University, Shanghai 200092, P. R. China.

[b] State Key Laboratory of Pollution Control and Resources Reuse, Shanghai Institute of Pollution Control and Ecological Security, School of Environmental Science and Engineering, Tongji University, Shanghai 200092, P. R. China.

[c] College of Chemical Engineering, Zhejiang University of Technology, Hangzhou 310014, P. R. China.

[d] key Laboratory for Green Chemical Process of Ministry of Education, School of Chemistry and Environmental Engineering, Wuhan Institute of Technology, 693 Xiongchun Road, Wuhan 430073, P. R. China.

***Corresponding Authors**

E-mail: lilc@tongji.edu.cn, liumx@tongji.edu.cn, ganlh@tongji.edu.cn

Table S1 Synthesis parameters and properties of quinone-amine polymer derived PCNs[a].

Samples	Effect factors	*T* (℃)	Ethanol (mL)	$n_{b/d}$	$W_{KOH/PNs}$	Size (nm)	S_{BET} ($m^2\ g^{-1}$)	N (wt.%)	O (wt.%)	C_m ($F\ g^{-1}$)
PCN_{600}	*T*	600	200	3	1	380	1620	11.64	10.41	186
PCN_{700}		700	200	3	1	380	2660	10.95	10.37	358
PCN_{800}		800	200	3	1	380	2218	6.15	12.66	267
PCN_{900}		900	200	3	1	380	1527	4.99	8.78	241
PCN-1	Solvent	700	100	3	1	550	1673	8.57	10.78	256
PCN-2		700	150	3	1	510	2144	7.22	9.56	295
PCN-3		700	250	3	1	350	2308	5.76	15.20	275
PCN-4	Monomer	700	200	1	1	340	2536	6.83	15.62	224
PCN-5		700	200	2	1	450	2365	7.89	16.40	279
PCN-6		700	200	6	1	530	2714	5.87	10.45	268
PCN-7	Activation	700	200	3	0	380	433	12.06	16.71	208
PCN-8		700	200	3	0.5	380	1562	11.23	12.48	245
PCN-9		700	200	3	2	380	3112	5.65	9.98	258

[a]*T*: carbonization/activation temperature; $n_{b/d}$: the molar ratio of *p*-benzoquinone to 3, 3'-diaminobenzidine; $W_{KOH/PNs}$: the mass ratio of KOH to polymer nanospheres; S_{BET}: specific surface area; N: nitrogen contents of PCNs; C_m: gravimetric specific capacitance of PCN electrodes measured in three-electrode system at 1 A g^{-1} using KOH electrolyte.

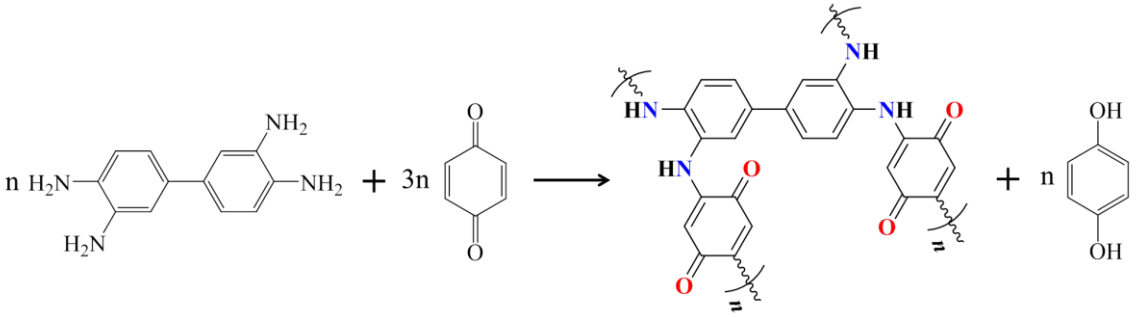

Scheme S1 Reaction process of 3, 3'-diaminobenzidine and *p*-benzoquinone in ethanol.

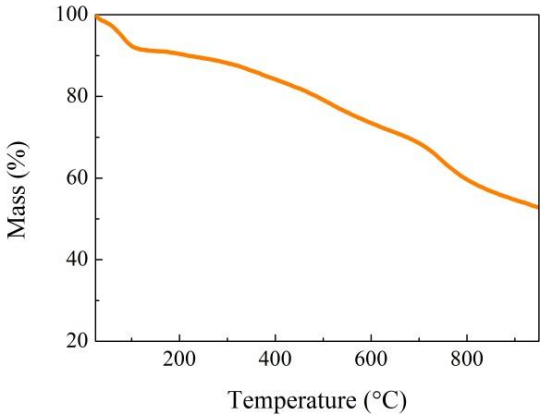

Fig. S1 TGA curve of quinone-amine polymer nanospheres in N_2 atmosphere.

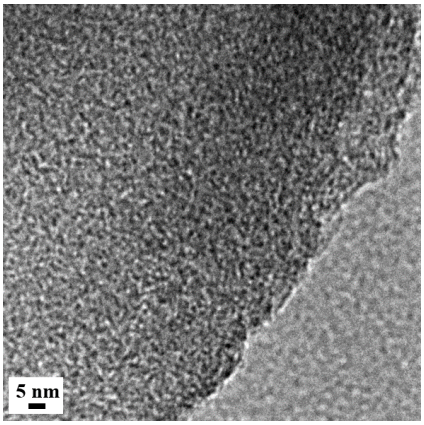

Fig. S2 A typical TEM image of PCN_{700}.

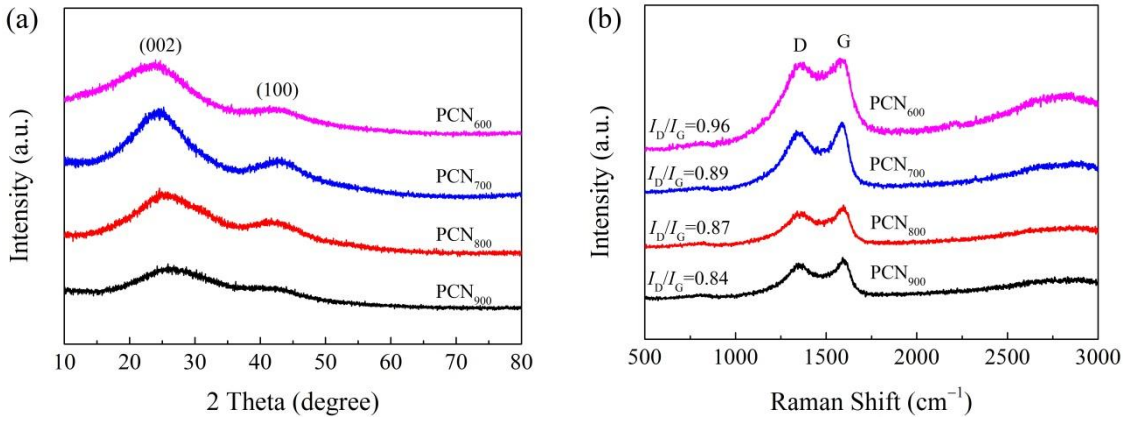

Fig. S3 (a) XRD patterns and (b) Raman spectra of PCNs.

Table S2 Comparison of surface areas (S_{BET}), nitrogen contents, specific capacitances (C_m) under different current densities (I_m) of reported heteroatom-doped carbon electrodes tested in 6 M KOH on a three-electrode system for supercapacitors in the literatures.

Materials	S_{BET} ($m^2\ g^{-1}$)	N (wt.%)	C_m ($F\ g^{-1}$)	I_m ($A\ g^{-1}$)	Ref.
N-doped 3D graphene networks	583	15.8	380	0.6	1
Carbon nitride	1356	15.3	372	1	2
N-doped carbon nanocages	1794	7.9	313	1	3
N-doped 2D polymers	594	4.04	233	1	4
N-doped carbon nanosheets	358	5.07	358	0.1	5
N-doped activated carbon	2900	3.98	185	0.4	6
N-doped graphene	–	2.51	280	1	7
N-doped carbon microspheres	1147	2.4	219	1	8
N-doped strutted graphene	1005	1.82	250	1	9
N-doped carbons	329	13.44	374	0.1	10
N-doped porous carbons	2096	7.2	262	0.2	11
N-doped graphene	–	4.2	312	0.1	12
N-doped carbon nanosheets	2494	4.7	242	0.1	13
N-doped carbon nanospheres	631	8.23	146	1	14
N-doped graphdiyne	679	3.67	250	0.2	15
PCN_{700}	2660	10.95	376	0.5	This
			358	1	work

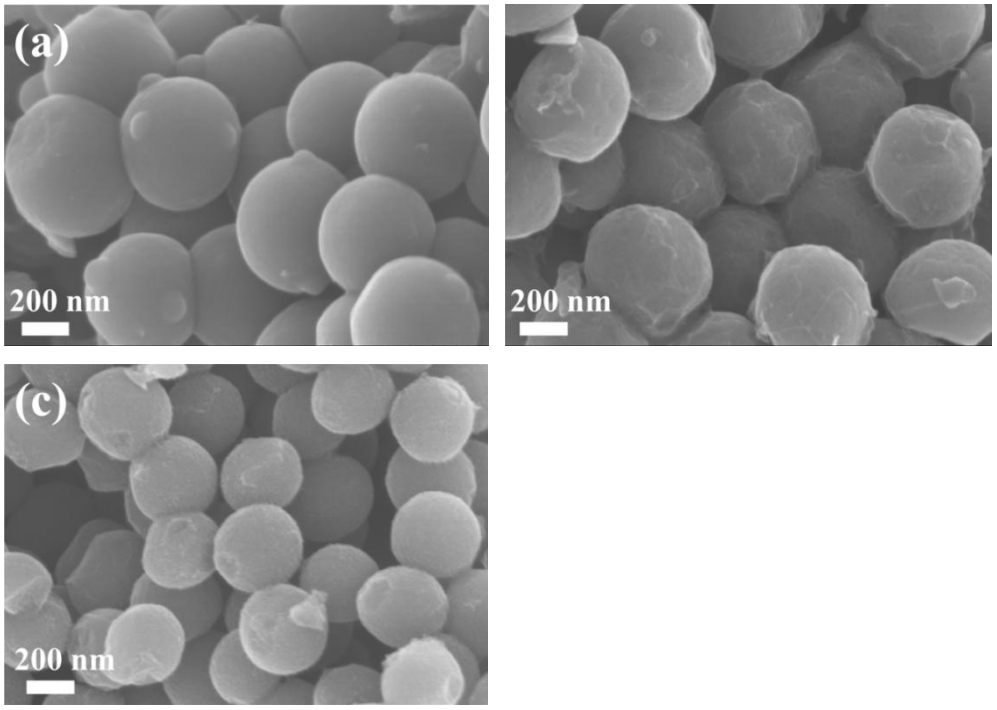

Fig. S4 SEM images of (a) PCN-1, (b) PCN-2 and (c) PCN-3.

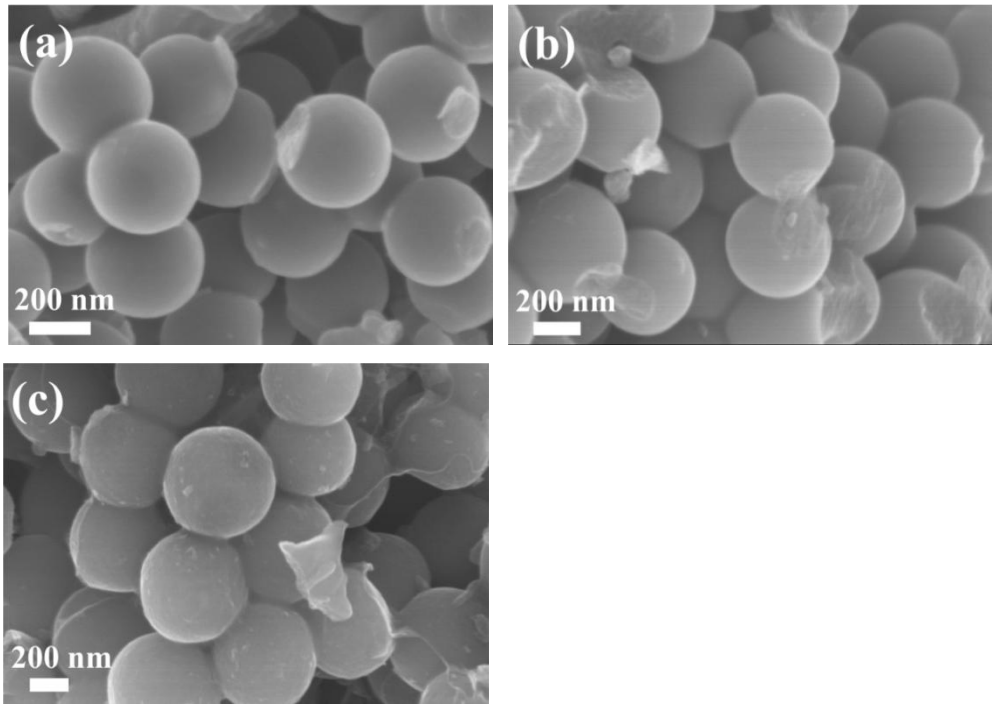

Fig. S5 SEM images of (a) PCN-4, (b) PCN-5 and (c) PCN-6.

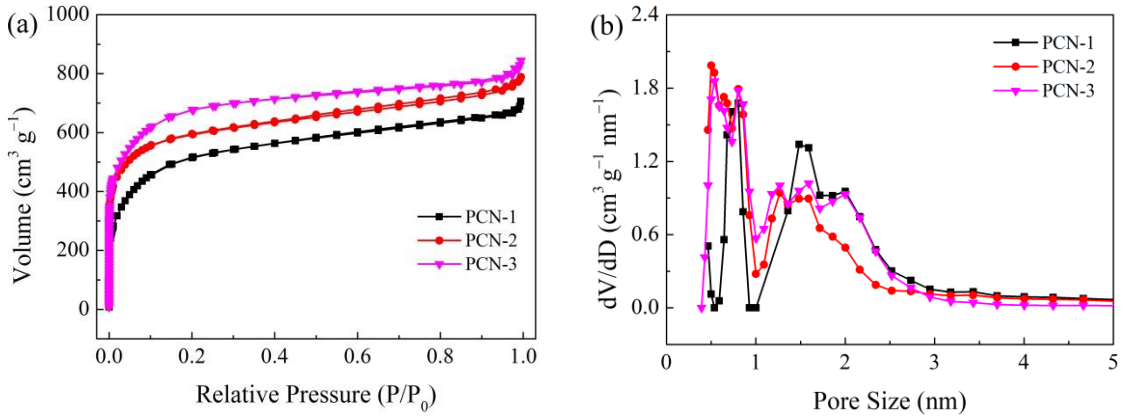

Fig. S6 (a) N_2 adsorption/desorption isotherms and (b) pore size distribution curves of PCN-1, PCN-2 and PCN-3.

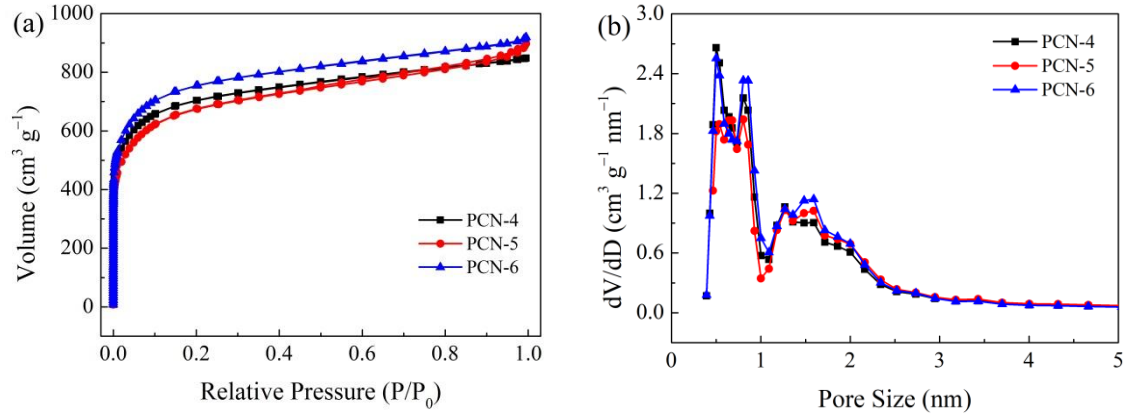

Fig. S7 (a) N_2 adsorption/desorption isotherms and (b) pore size distribution curves of PCN-4, PCN-5 and PCN-6.

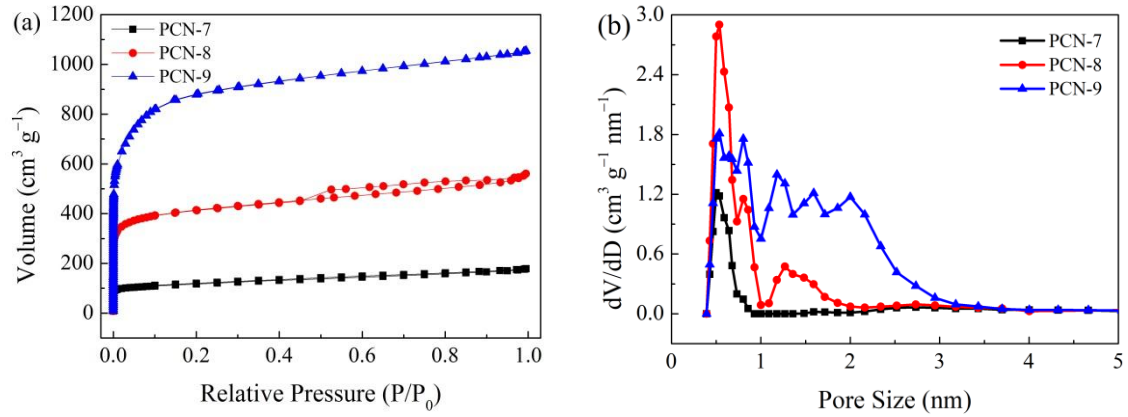

Fig. S8 (a) N_2 adsorption/desorption isotherms and (b) pore size distribution curves of PCN-7, PCN-8 and PCN-9.

Table S3 Pore structure parameters of PCNs.

Samples	S_{BET} (m^2 g^{-1})	$S_{Micropore}$ (m^2 g^{-1})	V_{total} (cm^3 g^{-1})	$V_{micropore}$ (cm^3 g^{-1})
PCN_{600}	1620	1331	0.98	0.62
PCN_{700}	2660	2422	1.54	1.19
PCN_{800}	2218	1938	1.36	0.98
PCN_{900}	1527	1285	1.01	0.70
PCN-1	1673	1389	1.07	0.71
PCN-2	2144	1859	1.21	0.82
PCN-3	2308	2134	1.29	1.01
PCN-4	2536	2264	1.31	1.01
PCN-5	2365	2027	1.38	0.94
PCN-6	2714	2432	1.42	1.09
PCN-7	433	325	0.27	0.14
PCN-8	1562	1118	0.86	0.45
PCN-9	3112	2788	1.63	1.27

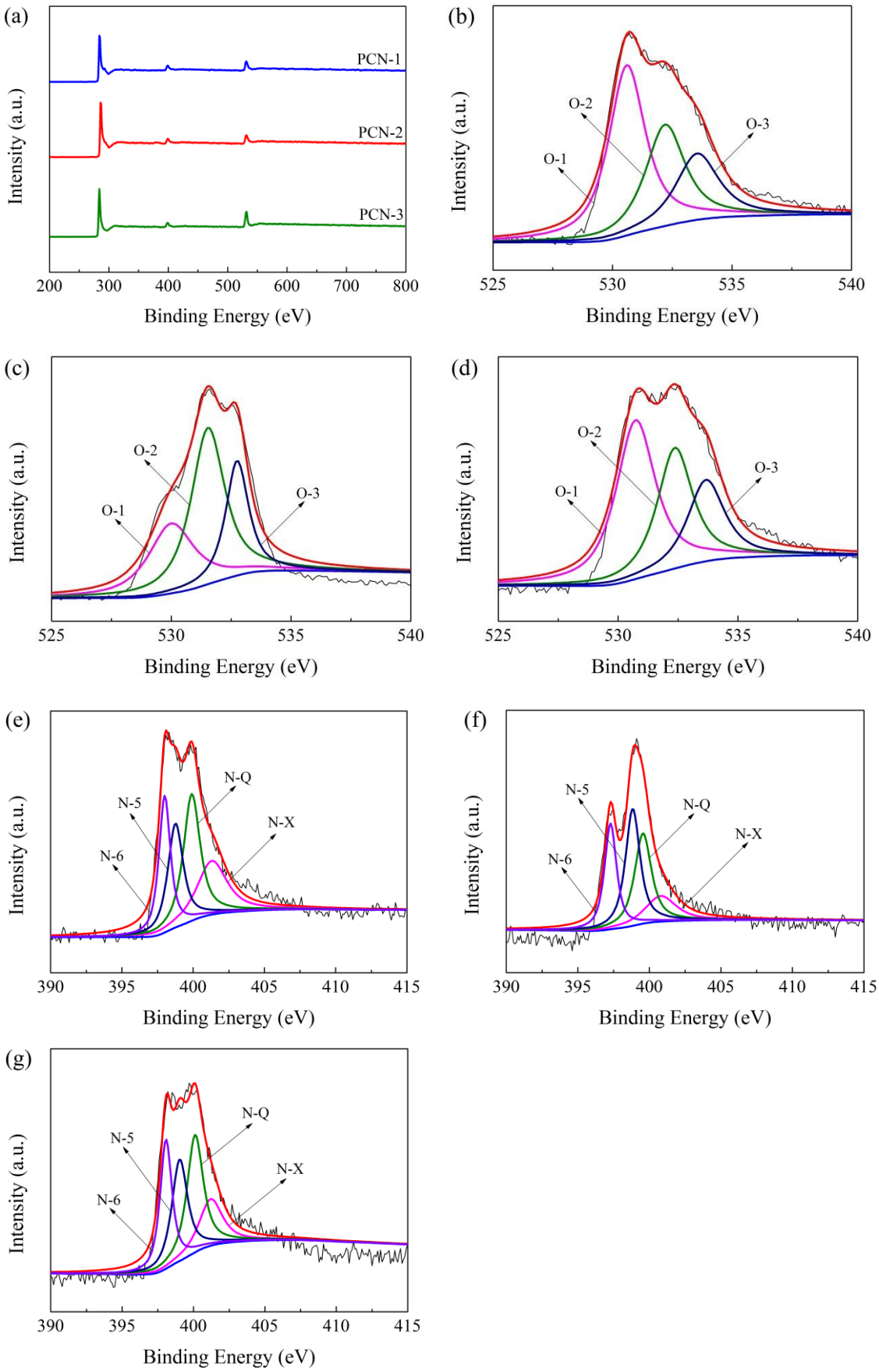

Fig. S9 (a) Wide-scan XPS spectra and (b–g) the fitted high-solution XPS spectra of O 1s and N 1s for (b, e) PCN-1, (c, f) PCN-2 and (d, g) PCN-3.

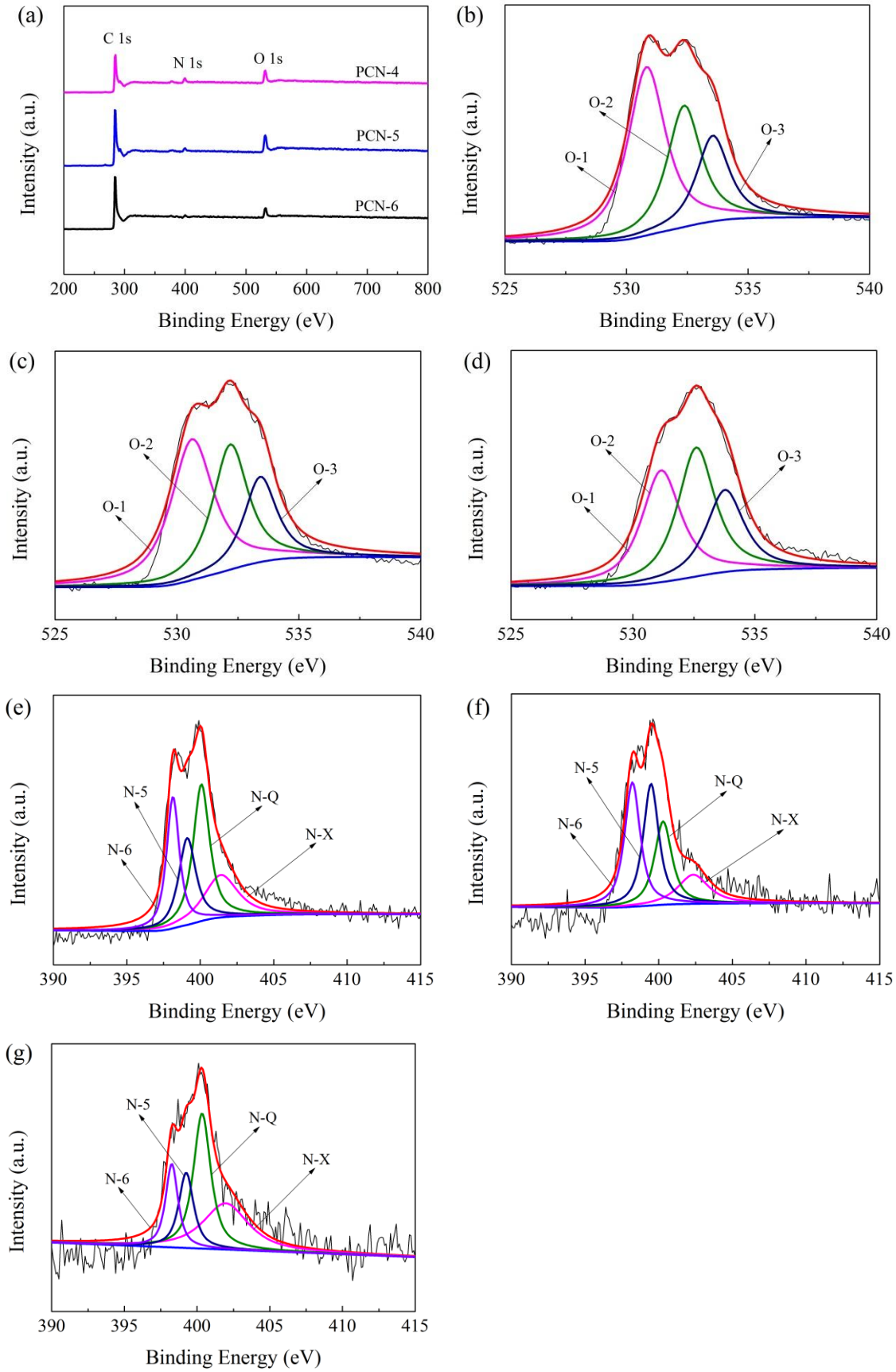

Fig. S10 (a) Wide-scan XPS spectra and (b–g) the fitted high-solution XPS spectra of O 1s and N 1s for (b, e) PCN-4, (c, f) PCN-5 and (d, g) PCN-6.

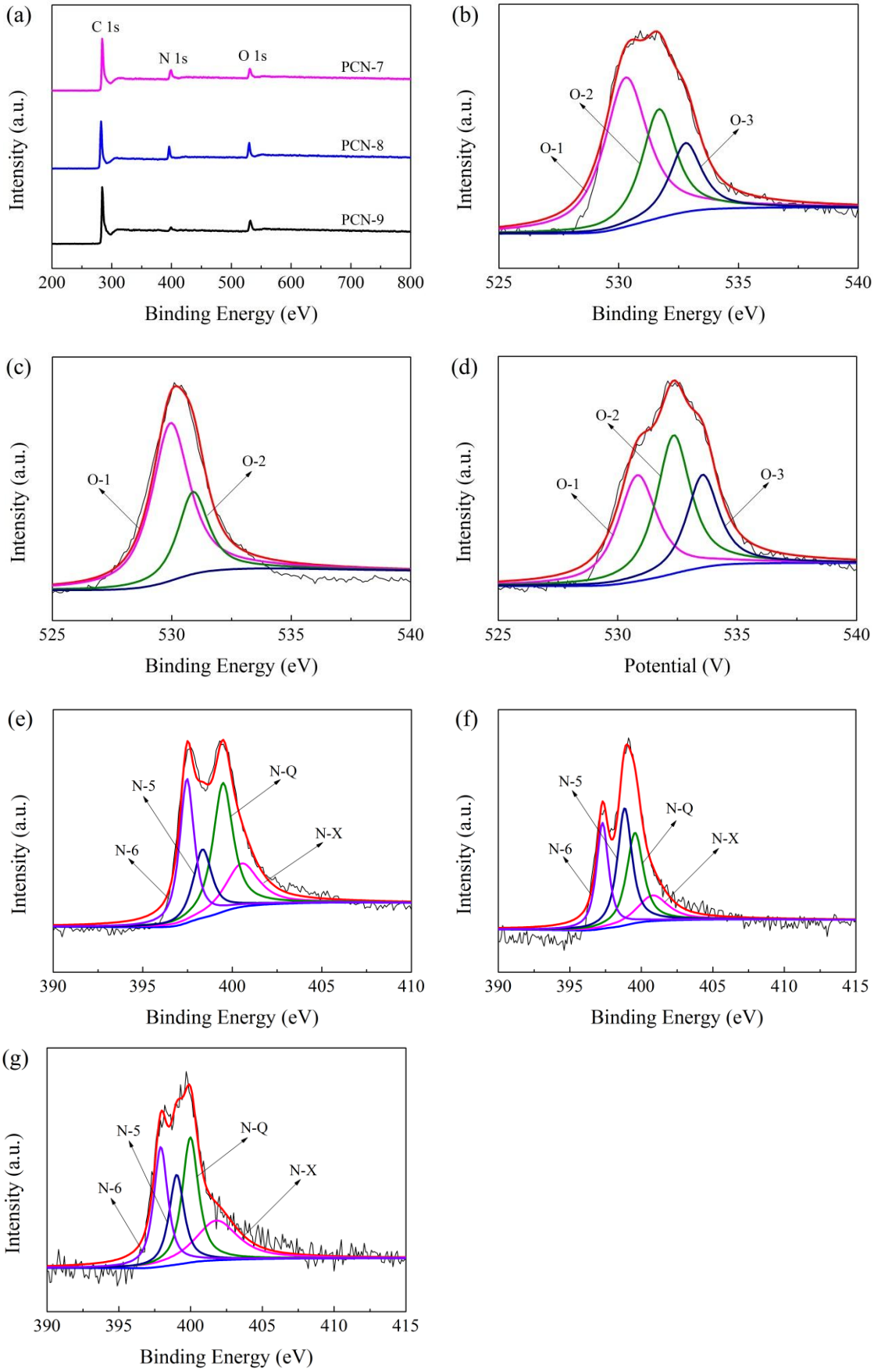

Fig. S11 (a) Wide-scan XPS spectra and (b–g) the fitted high-solution XPS spectra of O 1s and N 1s for (b, e) PCN-7, (c, f) PCN-8 and (d, g) PCN-9.

Table S4. Elemental compositions, relative contents of N and O species to N 1s and O 1s in PCNs.

Samples	C (wt.%)	N (wt.%)	O (wt.%)	N-6 (%) 398.2 eV	N-5 (%) 399.5 eV	N-Q (%) 400.3 eV	N-X (%) 401.6 eV	O-1 (%) 530.7 eV	O-2 (%) 532.1 eV	O-3 (%) 533.6 eV
PCN_{600}	77.94	11.64	10.41	39.92	16.99	24.73	18.36	27.76	46.37	25.87
PCN_{700}	78.68	10.95	10.37	32.59	15.84	26.92	24.65	38.69	38.04	23.27
PCN_{800}	81.19	6.15	12.66	24.22	16.63	30.50	28.65	23.29	40.02	36.69
PCN_{900}	86.23	4.99	8.78	24.41	14.98	38.58	22.03	31.23	41.49	27.28
PCN-1	80.65	8.57	10.78	22.75	23.24	30.76	23.25	47.92	30.43	21.65
PCN-2	83.22	7.22	9.56	24.23	32.21	28.62	14.94	29.17	47.09	23.74
PCN-3	79.04	5.76	15.20	25.16	26.15	30.98	17.71	46.55	31.41	43.27
PCN-4	84.00	6.83	9.17	24.51	21.68	32.97	20.84	48.03	31.09	20.88
PCN-5	75.72	7.89	16.40	31.50	30.61	23.41	14.48	45.51	33.48	21.01
PCN-6	83.67	5.87	10.45	15.76	16.97	35.65	31.62	35.90	39.07	25.02
PCN-7	71.23	12.06	16.71	28.45	17.42	34.75	19.38	52.52	29.74	17.74
PCN-8	76.28	11.23	12.48	24.23	32.21	28.62	14.94	70.64	29.36	–
PCN-9	84.37	5.65	9.98	24.99	19.95	30.05	25.01	35.07	39.93	25.00

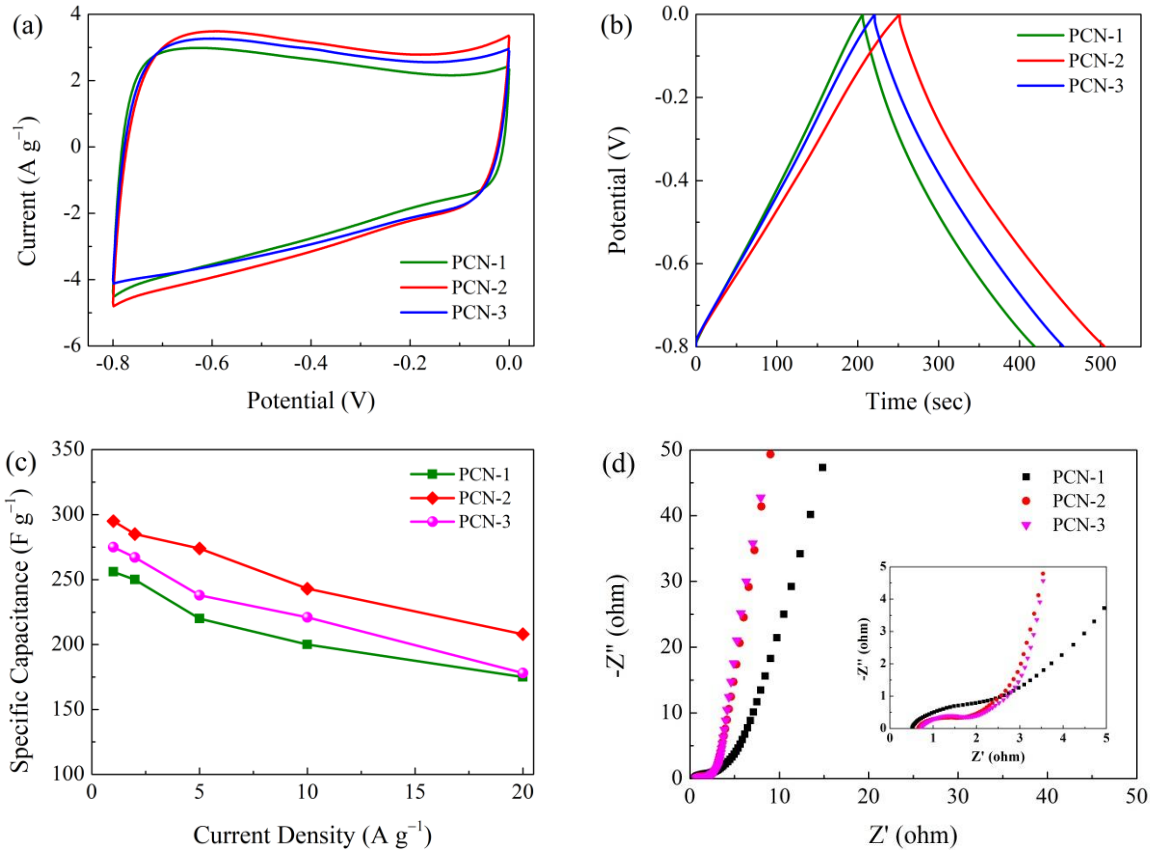

Fig. S12 (a) CV curves at 10 mV s^{-1}, (b) GCD curves at 1 A g^{-1}, (c) comparison of capacitances between the samples at different current densities, and (d) Nyquist plots of PCN-1, PCN-2 and PCN-3 electrodes in 6 M KOH electrolyte solution.

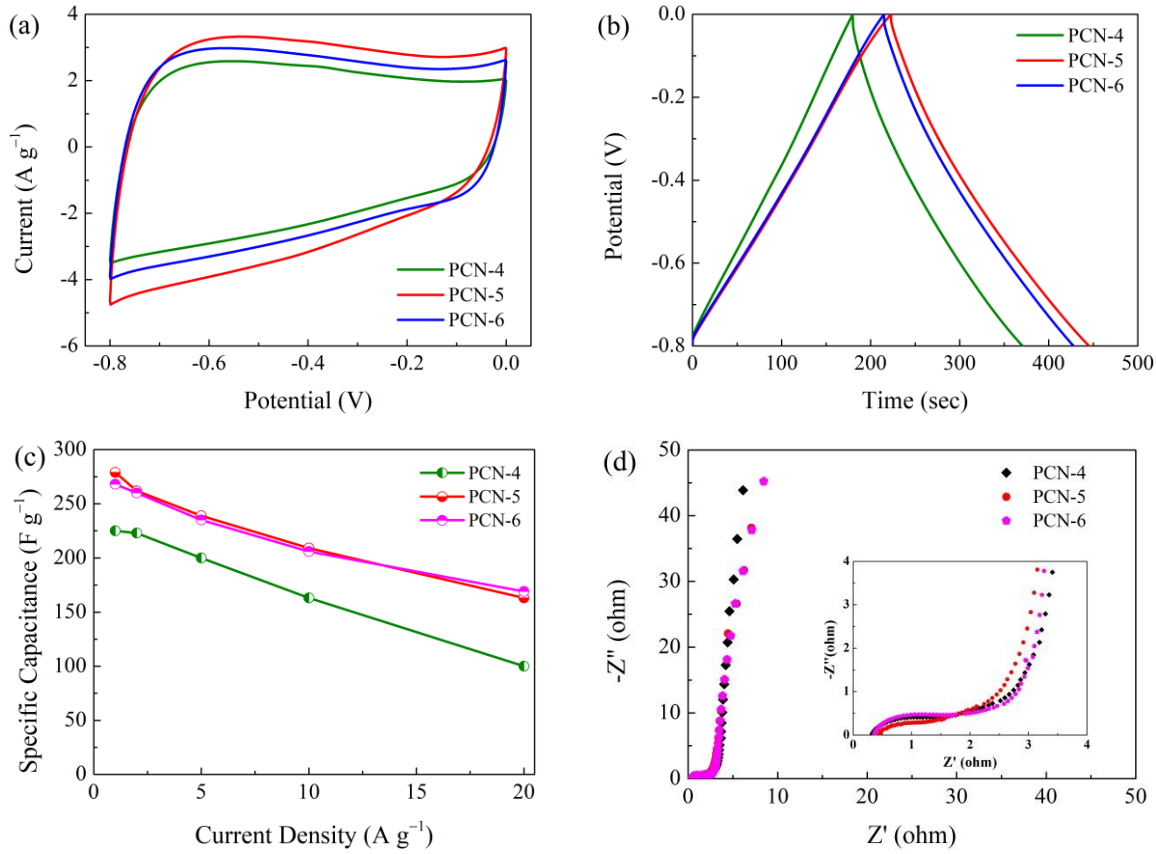

Fig. S13 (a) CV curves at 10 mV s^{-1}, (b) GCD curves at 1 A g^{-1}, (c) comparison of capacitances between the samples at different current densities, and (d) Nyquist plots of PCN-4, PCN-5 and PCN-6 electrodes in 6 M KOH electrolyte solution.

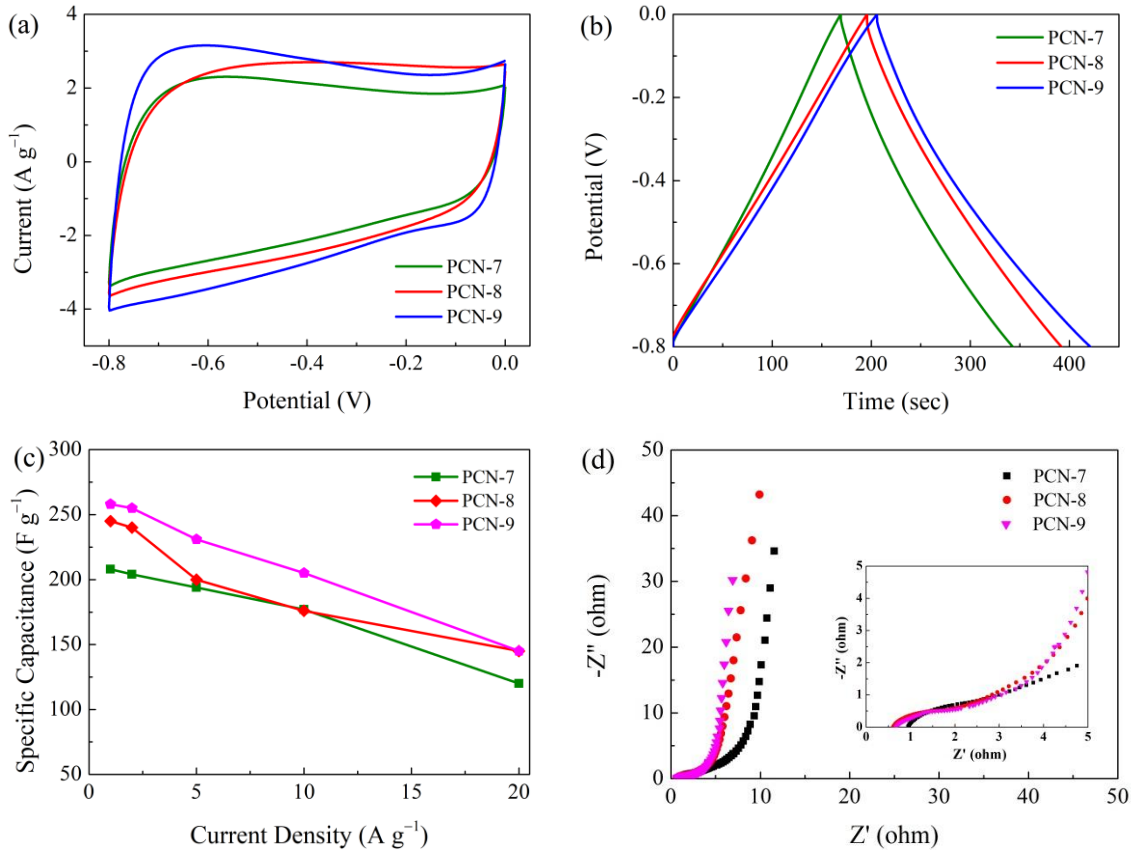

Fig. S14 (a) CV curves at 10 mV s^{-1}, (b) GCD curves at 1 A g^{-1}, (c) comparison of capacitances between the samples at different current densities, and (d) Nyquist plots of PCN-7, PCN-8 and PCN-9 electrodes in 6 M KOH electrolyte solution.

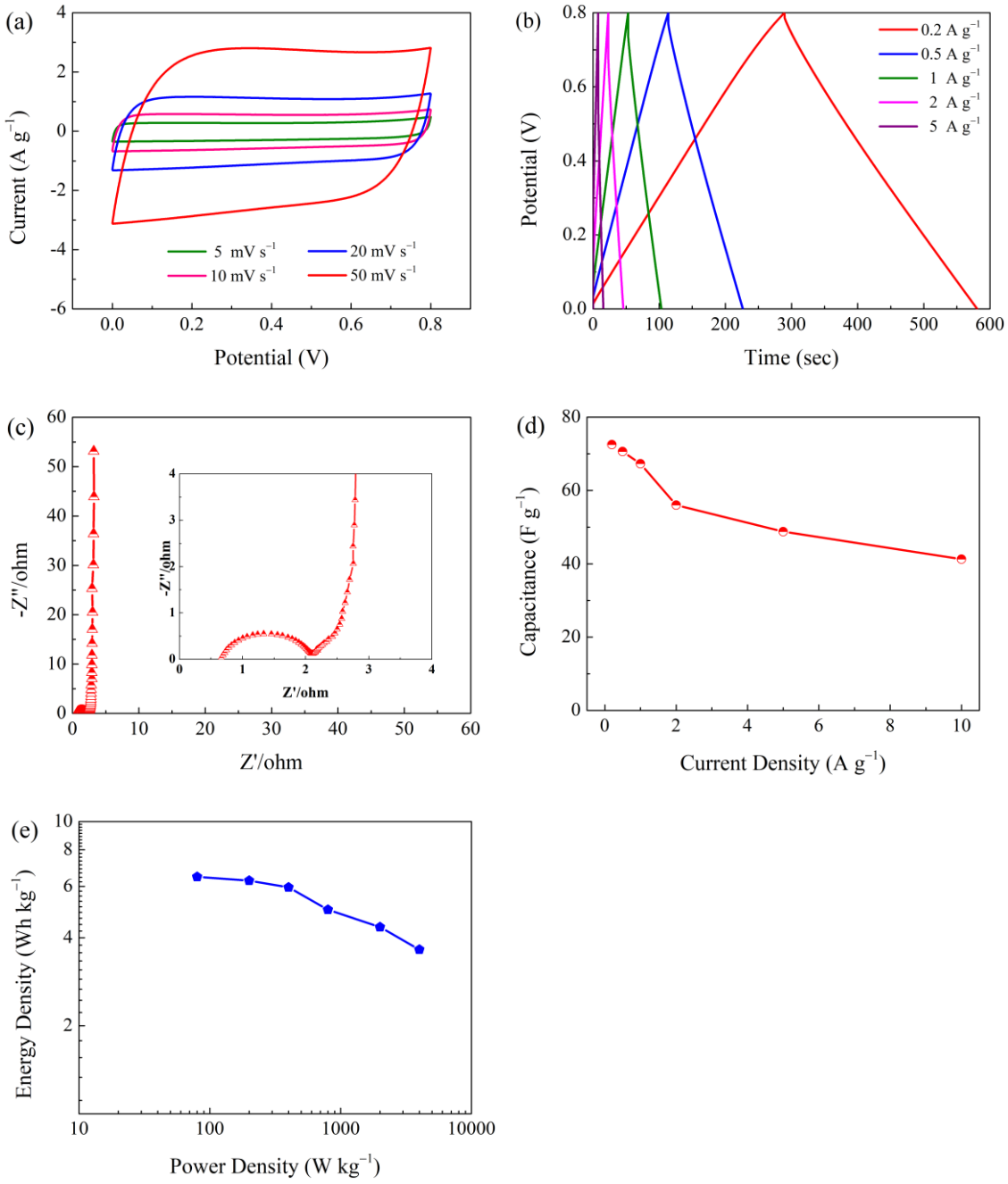

Fig. S15 The electrochemical performances of the assembled symmetric two-electrode coin-typed cell based on PCN electrodes and 6 M KOH electrolyte: (a) CV curves at different scann rates from 5 to 50 mV s^{-1}; (b) GCD curves at various current densities from 0.2 to 5 A g^{-1}; (c) Nyquist plots; (d) Gravimetric capacitances at different current densities; (e) Ragone plots.

References

1 W. Zhang, C. Xu, C. Ma, G. Li, Y. Wang, K. Zhang, F. Li, C. Liu, H. M. Cheng, Y. Du, N. Tang, W. Ren, *Adv. Mater.*, 2017, **29**, 1701677.

2 J. Xu, F. Xu, M. Qian, F. Xu, Z. Hong, F. Huang, *Adv. Mater.*, 2017, **29**, 1701674.

3 J. Zhao, H. Lai, Z. Lyu, Y. Jiang, K. Xie, X. Wang, Q. Wu, L. Yang, Z. Jin, Y. Ma, J. Liu, Z. Hu, *Adv. Mater.*, 2015, **27**, 3541−3545.

4 W. Liu, M. Ulaganathan, I. Abdelwahab, X. Luo, Z. Chen, S. J. Rong Tan, X. Wang, Y. Liu, D. Geng, Y. Bao, J. Chen, K. P. Loh, *ACS Nano*, 2018, **12**, 852−860.

5 Z. Ling, Z. Wang, M. Zhang, C. Yu, G. Wang, Y. Dong, S. Liu, Y. Wang, J. Qiu, *Adv. Funct. Mater.*, 2016, **26**, 111−119.

6 B. Li, F. Dai, Q. Xiao, L. Yang, J. Shen, C. Zhang, M. Cai, *Energy Environ. Sci.*, 2016, **9**, 102−106.

7 H. M. Jeong, J. W. Lee, W. H. Shin, Y. J. Choi, H. J. Shin, J. K. Kang, J. W. Choi, *Nano Lett.* 2011, **11**, 2472−2477.

8 B. Duan, X. Gao, X. Yao, Y. Fang, L. Huang, J. Zhou, L. Zhang, *Nano Energy*, 2016, **27**, 482−491.

9 X. Wang, Y. Zhang, C. Zhi, X. Wang, D. Tang, Y. Xu, Q. Weng, X. Jiang, M. Mitome, D. Golberg, Y. Bando, *Nat. Commun.*, 2013, **4**, 2905.

10 J.-S. M. Lee, M. E. Briggs, C.-C. Hu, A. I. Cooper, *Nano Energy*, 2018, **46**, 277−289.

11 L. Estevez, R. Dua, N. Bhandari, A. Ramanujapuram, P. Wang, E. P. Giannelis, *Energy Environ. Sci.*, 2013, **6**, 1785.

12 K. Wang, M. Xu, Y. Gu, Z. Gu, J. Liu, Q. H. Fan, *Nano Energy*, 2017, **31**, 486−494.

13 J. Hou, C. Cao, F. Idrees, X. Ma, *ACS Nano*, 2015, **9**, 2556−2564.

14 C. Wang, F. Wang, Z. Liu, Y. Zhao, Y. Liu, Q. Yue, H. Zhu, Y. Deng, Y. Wu, D. Zhao, *Nano Energy*, 2017, **41**, 674−680.

15 H. Shang, Z. Zuo, H. Zheng, K. Li, Z. Tu, Y. Yi, H. Liu, Y. Li, Y. Li, *Nano Energy*, 2018, **44**, 144−154.